IOP Conf. Series: Materials Science and Engineering **735** (2020) 012020 doi:10.1088/1757-899X/735/1/012020

# Microstructures, Optical Properties and Degradation Efficiency of Nitrogen-doped Titanium Dioxide to Automobile Exhaust

**Zhihui Hu[1, 2], Wei Liu[1, 3], Tao Xu[1, 2*] and Xiaoyan Li[1, 3]**

1 National Engineering Laboratory for Advanced Road Materials, 2200 Chengxin Avenue, Nanjing 211112, Jiangsu, China
2 College of Civil Engineering, Nanjing Forestry University, 159 Longpan Road, Nanjing 210037, Jiangsu, China
3 JSTI Group, 2200 Chengxin Avenue, Nanjing 211112, Jiangsu, China
*****Corresponding author E-mail: seuxt@163.com

**Abstract.** To understand the influence of nitrogen (N) dopant on phase structure, morphology, optical property, photocatalytic degradation of $TiO_2$ to automobile exhaust (AE) under visible light irradiation, the N-doped $TiO_2$ was first prepared, and then X-ray diffraction (XRD), transmission electron microscopy (TEM), ultraviolet-visible light diffuse reflectance spectra (UV-vis DRS) and photocatalytic degradation tests were conducted. Results indicated that only anatase phase was found in both pure $TiO_2$ and N-doped $TiO_2$, and the N doping improved the dispersity of $TiO_2$. Also, the N doping increased the absorbance of $TiO_2$ under UV and visible light, respectively. An obvious red shift was observed on UV-Vis DRS of pure and N-doped $TiO_2$ samples, indicating that the spectral response range of $TiO_2$ was expanded to visible light region, and the utilization efficiency of solar irradiance was increased. The prepared N-doped $TiO_2$ nanoparticles with an N dopant content of 3.0% showed better optical properties. Finally, the N doping improved the photocatalytic activity of $TiO_2$ to AE in the visible light region. Furthermore, the N-doped $TiO_2$ presented lower degradation efficiency to CO than that to $CO_2$ under visible light radiation. Thus, it is found that the degradation efficiency of $TiO_2$ to AE can be increased by the N doping under visible light radiation.

## 1. Introduction

Automobile exhaust (AE) including $NO_x$, HC, $CO_2$, CO, etc. causes serious environmental pollution [1]. AE brings great harms to human health and ecological environments so that some photocatalytic technologies have been developed to purify AE. Among them, $TiO_2$, as one of important photocatalysts, is utilized to chemically degrade AE and other air pollutants due to its advantages of high photoactivity, good stability, non-toxicity, low cost, etc [2].

However, owing to the high band gap energy of $TiO_2$, it can only be excited by ultraviolet (UV) light in sunlight to exert the property of photocatalytic degradation. However, the UV light onlu occupies about 4% in the total solar radiation [3]. This not only causes the insufficient use of solar energy but also lowers the photocatalytic efficiency of $TiO_2$. Another disadvantage of pure $TiO_2$ is that the recombination of photo-generated carriers decreases the photocatalytic activity of $TiO_2$ [4]. Therefore, it is meaningful to increase the photocatalytic efficiency of $TiO_2$ under visible light which occupies about 45% of total solar radiation.

Currently, the transition metal or nonmetal doping can not only broaden the photoresponse range of

$TiO_2$, but also promote the generation of electron holes. It has become one of the important methods to improve the photocatalytic efficiency of $TiO_2$ [5]. Among them, the N-doped $TiO_2$ has been paid more efforts due to its lower preparation cost and high photocatalytic activity under visible light, and controllable synthesis [6]. The photocatalytic performances of N-doped $TiO_2$ to methylene blue under the irradiation of visible light were discussed by Ramchiary et al. [7]. Powell [8] used the N doping method of $TiO_2$ to increase the absorbance of visible light, improving the photocatalytic activity of $TiO_2$. Todorova [9] reported the N-doped $TiO_2$ showed higher degradation efficiency to $NO_x$ than pure $TiO_2$. Triantis et al. [10] claimed that energy states in N doping configuration were formed in the $TiO_2$ band gap.

Additionally, it is noted that the photocatalytic degradation mechanism of N-doped $TiO_2$ under the radiation of visible light has not been well understood. Also, few researches have been focused on photocatalytic degradation efficiency of N-doped $TiO_2$ nanoparticles to AE. The purpose of this study is to use the N element as a dopant for doping $TiO_2$, improving the degradation efficiency of $TiO_2$ to AE under visible light. For this, in this study, the N-doped $TiO_2$ nanoparticles were synthesized using the sol-gel method. Then the phase microstructure of prepared $TiO_2$ nanoparticles were tested using X-ray diffraction (XRD), and the micromorphology and dispersity of N-doped $TiO_2$ nanoparticles were characterized by the transmission electron microscopy (TEM). In addition, the optical performance of $TiO_2$ nanoparticles were analyzed by ultraviolet-visible light diffuse reflectance spectra (UV-vis DRS). Finally, the degradation tests were conducted to validate the photocatalytic activity of N-doped $TiO_2$ to AE under visible light.

## 2. Materials and Method

### *2.1. Synthesis of $TiO_2$ Samples*

N-doped $TiO_2$ nanoparticles were prepared using the sol-gel method. The tetra-n-butyl titanate and carbamide were utilized as titanium and N precursor, respectively. Firstly, 17 mL tetra-n-butyl titanate and 30 mL absolute ethanol were blended for 30 min at room temperature, preparing the solution A. Secondly, 8 mL deionized water, 20 mL acetic acid and 28 mL anhydrous alcohol were stirred, and then a calculated amount of carbamide (the mole ratio of N/Ti was 1.0%, 2.0%, 3.0% and 4.0%, respectively.) were dropped and fully mixed, preparing the solution B.

Then, the solution B was slowly dropped into solution A, and was stirred using a magnetic stirrer at 30 $^oC$, thus the transparent and uniform sol was obtained, and the sol was matured at room temperature for 7 days to prepare the gel. After that, the prepared gel was dried at 80 $^oC$ for 1 day, and was milled into powders and calcined at 400 $^oC$ for 2.5 h. The N-doped $TiO_2$ nanoparticles were obtained. The prepared samples were marked as $TiO_2$+NX (the X was the N dopant content). Based on the same approach, N-doped $TiO_2$ samples containing various N dopant contents were synthesized. However, the pure $TiO_2$ nanoparticles were synthesized without the carbamide in the mixed liquor in the second step.

### *2.2. Characterization Methods*

The phase structures of prepared $TiO_2$ samples were tested by XRD (Ultima IV type, Rigaku, Japan) with a Cu-$K\alpha$ radiation ($\lambda$=0.15418 nm). XRD patterns were recorded in the $2\theta$ range of 10° - 80°at a rate of 2°/min. The applied current was 30 mA, and the accelerating voltage was 40 kV.

A field emission TEM (JEM-2100 (HR) type, JEOL, Japan) was utilized to characterized microstructures and morphology of $TiO_2$. Its lattice resolution was 0.14 nm, and the amplification times were 50-1500000, and the point resolution was 0.23 nm.

The DRS of $TiO_2$ samples were recorded by a UV-vis spectrophotometer (Lambda 950 type, PE, USA) coupled with an integrating sphere. The scanning range was 200–800 nm at a data interval of 1nm. The reference sample for baseline correction was $BaSO_4$ standard.

### *2.3. Photocatalytic Activity Tests*

As shown in Fig.1, an experimental setup was used to validate the photocatalytic degradation efficiency of prepared $TiO_2$ to AE under visible light. The prepared $TiO_2$ samples were first evenly

scattered on a plate with 300 mm in both length and width, and then the plate was placed in the closed non-transparent reactor. The height of incandescent lamp was about 20 cm from the plate. AE was produced by a gasoline engine generator. Its exhaust pipe was connected with the closed reaction reactor. The degradation tests of $TiO_2$ to four constituents of AE were carried out under visible light. A vacuum pump connected to the reaction reactor was utilized to control the initial pressure of the closed reaction reactor.

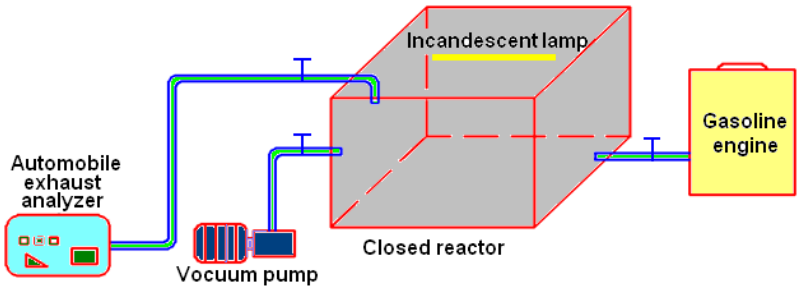


**Figure 1.** Schematic Diagram of Test Setup of Photocatalytic Degradation

Firstly, the vacuum pump started to run for 60 s. The gasoline engine was then started to produce AE until it run steadily. The intake valve was opened, and AE was introduced into the closed reaction reactor. The intake valve was closed when the initial content of each constituent of AE approached a stable value.

After that, the incandescent lamp was turned on to validate the photocatalytic activity of $TiO_2$ to each constituent of AE. The content change of each constituent of AE vs. the radiation time was recorded for 60 min by an AE analyzer (HPC506 type, Huapeng, China). In the radiation process of incandescent lamp, the contents of $NO_x$, CO, HC and $CO_2$ were tested at the interval of 10 min.

Finally, the degradation efficiency of $TiO_2$ to each constituent of AE was taken as the evaluating index calculated by Eq. (1).

$$\eta = (C_0\text{-}C_{end})/C_0 \quad (1)$$

Where, $C_0$ was the initial content of each constituent, and $\eta$ was the degradation efficiency, and $C_{end}$ was the residual content of each constituent at the end of degradation reaction.

## 3. Results and Discussion

### *3.1. Phase Structure*

XRD patterns of pure and N-doped $TiO_2$ are presented in Figure 2. As illustrated in Figure 2, the N-doped and pure $TiO_2$ samples show similar phase structures. The representative diffraction peaks are observed at 62.7°, 55.0°, 53.9°, 48.0°, 37.8° and 25.3°, which correspond to six crystal planes of (204), (211), (105), (200), (004) and (101), respectively. It is noticed that the typical diffraction peaks of the rutile phase of $TiO_2$ are not observed, and all N-doped $TiO_2$ samples show anatase phase based on the comparison with the JCPDS NO: 21-1272. This suggests that the synthesized $TiO_2$ samples have high purity and crystallinity.

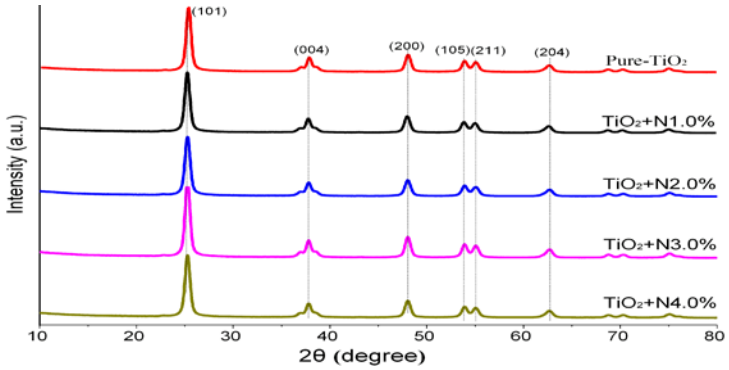


**Figure 2.** Typical XRD Patterns of N-doped and Pure $TiO_2$ Samples

By comparison, the phase compositions of N-doped $TiO_2$ samples are almost unchanged when compared with that of pure $TiO_2$ sample. Also, it is observed that the peak positions of major diffraction peaks of N-doped $TiO_2$ samples are similar with those of pure $TiO_2$ nanoparticles, but the above diffraction intensities are slightly changed. Moreover, the diffraction peaks of N impurities in the XRD diffraction patterns are not found. This suggests that the N dopants are evenly dispersed in the crystal lattices of $TiO_2$ samples, and its effects on the microstructures of $TiO_2$ are ignorable. Therefore, the crystal phase microstructures of $TiO_2$ nanoparticles are not changed by the N dopant.

### *3.2. Morphology Changes*

The influences of the N dopant on the morphology and dispersity of $TiO_2$ are analyzed by TEM images of pure and N-doped $TiO_2$ as illustrated in Figure 3. From Figure 3, the particle morphologies of pure and N-doped $TiO_2$ present no obvious changes, and still show the spherical nanoparticles. The crystallite sizes of pure and N-doped $TiO_2$ are in the range between 13 nm to 16 nm. This is consistent with the XRD test results. Additionally, the dispersity of $TiO_2$ nanoparticles is increased when the N dopant content is raised from 0 % to 4.0 %. This is because the N-doping lowers the $TiO_2$ agglomeration in the heat treatment process to increase the dispersibility of $TiO_2$ nanoparticles. Also, this improves the specific surface area of $TiO_2$ nanoparticles, which is beneficial to raise the photocatalytic degradation efficiency of N-doped $TiO_2$.

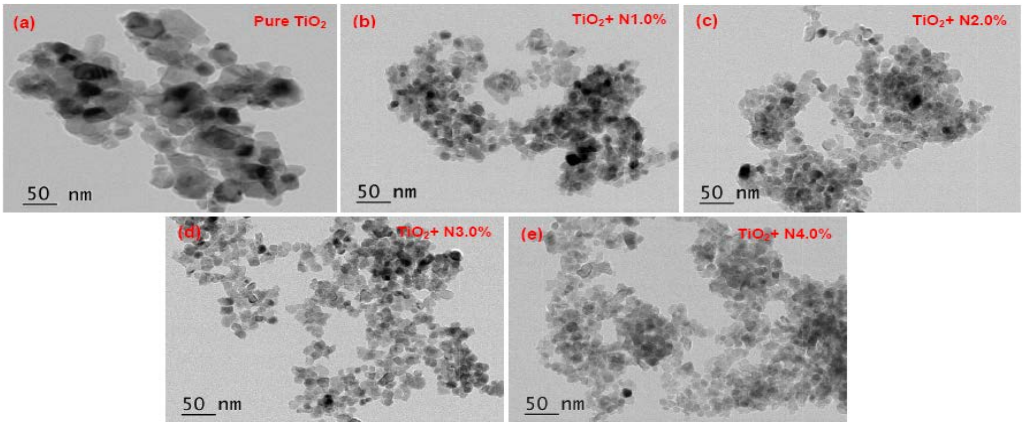


**Figure 3.** TEM Images of Pure and N-doped $TiO_2$ Nanoparticles

### *3.3. Optical Property*

In order to discuss effects of different N dopant contents on optical performances of $TiO_2$ nanoparticles, the test results of UV-vis DRS of N-doped and pure $TiO_2$ samples are provided in Figure 4.

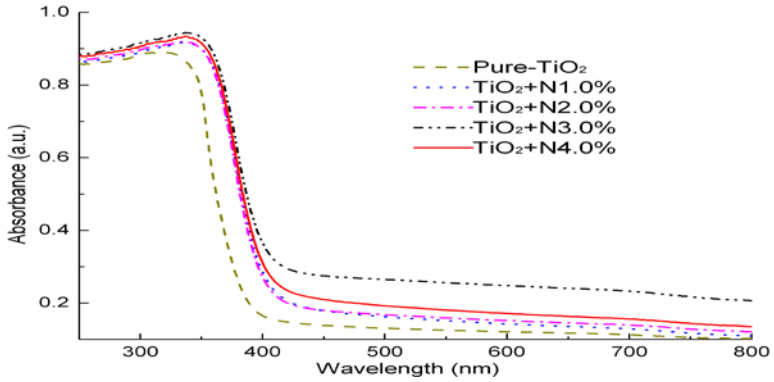


**Figure 4.** Test Results of UV-Vis DRS of N-doped and Pure $TiO_2$ Nanoparticles

It is seen from Figure 4 that the absorbance of N-doped $TiO_2$ is obviously improved under visible light radiation as compared with that of pure $TiO_2$ samples. Moreover, the optical absorption edges of N-doped $TiO_2$ present a red shift toward high wavelength, and the $TiO_2$+N3.0% shows the most obvious red shift toward high wavelength. This implies that the N-doping expands the optical absorption edge of $TiO_2$ from UV light to visible light region. This is conductive to increase the photocatalytic degradation efficiency and extend the utilization range of $TiO_2$ nanoparticles. The reason for this is that the local intermediate band gap (N2p) energy level is formed by the introduced N dopant on the top of O2p valence band in the $TiO_2$ nanoparticles [11]. Electrons of the doping energy level can be activated to the conduction band of $TiO_2$, resulting in the long wave photons to be absorbed [12]. Therefore, the absorption spectrum range of $TiO_2$ is expanded to the visible light region and the absorption performance in the visible light region is increased.

### *3.4. Photocatalytic Degradation Efficiency to AE under Visible Light*

Based on the above analysis results, it is found that $TiO_2$+N3.0% sample has better optical properties. Therefore, we only discussed the photocatalytic activity of $TiO_2$+N3.0% and pure $TiO_2$ to each constituent of AE under visible light. The changes in $NO_x$ and HC concentration are shown in Figure 5 during the photocatalytic degradation of $TiO_2$+N3.0% and pure $TiO_2$.

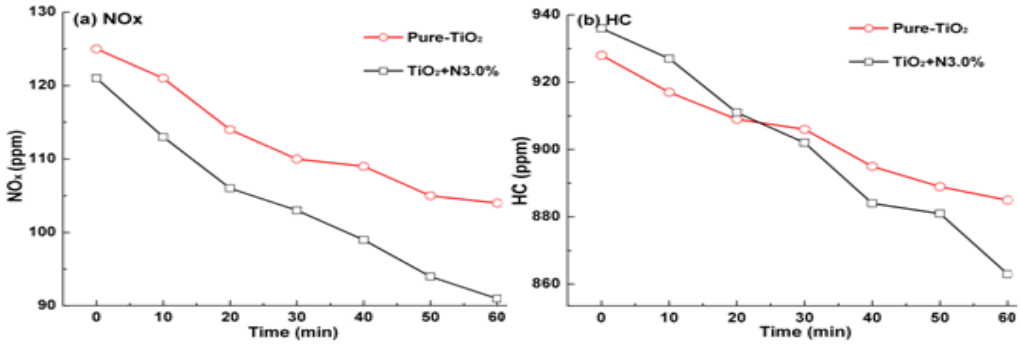


**Figure 5.** Concentration Changes of $NO_x$ and HC under Visible Light

It is found from Figure 5 (a) that the photocatalytic degradation of $TiO_2$+N3.0% and pure $TiO_2$ to $NO_x$ are similar in the first 30 min, and then the degradation effects of $TiO_2$+N3.0% is much higher than that of pure $TiO_2$. As presented in Fig.5 (b), $TiO_2$+N3.0% exhibits a better photocatalytic degradation performance to HC in the first 10 min, and then degradation effects of the two $TiO_2$ samples tend to be equal in the next 20 min, but $TiO_2$+N3.0% sample shows a better photocatalytic degradation performance in the last 30 min. This indicates that the N doping actually improves the photocatalytic degradation efficiency of $TiO_2$ to $NO_x$ and HC under visible light.

This is because the impurity levels in $TiO_2$ are produced due to the substitution of doped N for partial O element. The electronegativity differences between N and O element form oxygen vacancies

around the substituted position, leading to the crystal lattice distortion in $TiO_2$ [13]. This causes some defects to generate on the surface of crystal, thereby the recombination of photo-generated electrons and holes is inhibited and the photocatalytic active centers are increased simultaneously [14]. All these are beneficial to increase the photocatalytic degradation efficiency of $TiO_2$ to AE under visible light.

The changes in CO and $CO_2$ concentration are shown in Figure 6 during the photocatalytic degradation of $TiO_2$+N3.0% and pure $TiO_2$.

It is noted from Figure 6 (a) that the photocatalytic degradation efficiencies of $TiO_2$+N3.0% and pure $TiO_2$ to CO are not obviously improved on the whole, but the N-doped $TiO_2$ sample still presents a slightly higher photocatalytic degradation property to CO than that of pure $TiO_2$ sample. As illustrated in Figure 6 (b), the photocatalytic degradation efficiencies of $TiO_2$+N3.0% and pure $TiO_2$ to $CO_2$ are almost equal each other in the first 30 min, but the pure $TiO_2$ shows a lower degradation efficiency than that of $TiO_2$+N3.0% sample in the next 30 min.

This suggests that the photocatalytic activity of $TiO_2$+N3.0% to CO and $CO_2$ is higher than that of pure $TiO_2$ although the photocatalytic degradation efficiencies of $TiO_2$+N3.0% and pure $TiO_2$ samples to $CO_2$ and CO are not obviously increased. All these indicate that the N doping can increase the photocatalytic degradation efficiencies of $TiO_2$ to $CO_2$ and CO under visible light. The reasons for this are the band gap of $TiO_2$ is narrowed owing to the N doping, and the absorption range of $TiO_2$ to visible light is broadened to absorb more visible light energy and generate more electron holes [15]. Also, the electrons in activated state are more likely to jump and accelerate the transfer rate of electron interface, improving the photocatalytic degradation efficiency under visible light.

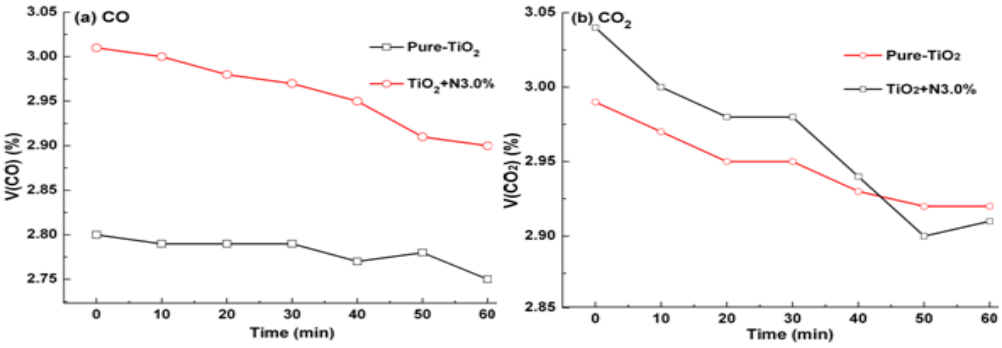


**Figure 6.** Concentration Changes of CO and $CO_2$ under Visible Light Irradiation

Table 1 provides the calculated results of photocatalytic degradation efficiencies of $TiO_2$+N3.0% and pure $TiO_2$ to each constituent of AE under visible light.

**Table 1.** Calculated Results of Photocatalytic Degradation Efficiencies of $TiO_2$+N3.0% and Pure $TiO_2$ to Each Constituent of AE

| $TiO_2$ samples | Photocatalytic degradation efficiency (%) | | | |
|---|---|---|---|---|
| | CO | $CO_2$ | HC | $NO_x$ |
| Pure-$TiO_2$ | 1.5 | 2.1 | 4.6 | 16.7 |
| $TiO_2$+N3.0% | 3.7 | 4.3 | 7.8 | 25.2 |

From Table 1, it is found that the pure $TiO_2$ has limited photocatalytic degradation efficiencies to different constituents of AE under visible light. However, the photocatalytic degradation efficiencies of N-doped $TiO_2$ to different constituents of AE under visible light are distinctly increased. It is concluded that the N doping is a feasible approach to increase the photocatalytic degradation efficiency of $TiO_2$ to AE under visible light.

## 4. Conclusions

(1) Only contain anatase phase is found in the prepared N-doped nanoparticles with a slight

distortion. As the N dopant content is raised from 0% to 4%, the dispersity of $TiO_2$ nanoparticles is increased, improving the specific surface area and photocatalytic degradation efficiency of $TiO_2$. The grain size range of $TiO_2$ sample is 13-16 nm with a spherical shape.

(2) N-doped $TiO_2$ show higher optical absorptions than pure $TiO_2$ in UV light and visible light regions. A red shift to higher wavelength is seen on UV-Vis DRS due to the N doping of $TiO_2$, leading to the decrease in band gap of $TiO_2$. This causes $TiO_2$ to absorb more visible light and increase the utilization efficiency of solar irradiance, increasing the degradation efficiency of $TiO_2$.

(3) The N doping improves the degradation efficiency and photocatalytic activity of $TiO_2$ to AE under visible light. The N-doped $TiO_2$ shows lower degradation efficiencies to $CO_2$ and CO than those to $NO_x$ and HC of AE. Also, the N-doped $TiO_2$ shows lower photocatalytic activity to CO than to $CO_2$.

(4) It is concluded that the N dopant improves the photocatalytic degradation efficiency of $TiO_2$ to each constituent of AE under visible light for air purification, and expands the application range of TiO2. These are beneficial to further develop the pollutant purification technology using N-doped $TiO_2$ nanoparticles as raw materials of building coating, road pavement, etc. along the street.

## 5. Acknowledgements

Authors would like to thank the financial support from Open Research Fund of National Engineering Laboratory for Advanced Road Materials, China (No. NLARMORF-2018-02), and China International Research Cooperation Projects (No. 2016YFE0108200), Research Project of Department of Transportation of Jiangsu, China (No. 2016 Y01, 2016Y03 and 2018Y25). Also, we would like to thank Advanced Analysis &Testing Center of Nanjing Forestry University for the assistance in experiments.

## 6. References

[1] Jin, J., Xiao, T., Tan, Y.Q. Effects of $TiO_2$ pillared montmorillonite nanocomposites on the properties of asphalt with exhaust catalytic capacity. J. Clean. Produt. 2018, 205: 339-349.

[2] Zhang, W.G., Zhang, Y.X., Jia, Z.R. Test method and material design of asphalt mixture with the function of photocatalytic decomposition of automobile exhaust. Constr. Build. Mater. 2019, 215: 298-309.

[3] Veluru, J.B., Appukuttan, S.N., Zhu, P.N. Synthesis and characterization of rice grains like Nitrogen-doped $TiO_2$ nanostructures by electrospinning–photocatalysis. Mater. Lett. 2011, 65 (19- 20): 3064.

[4] Daghrir, R., Drogui, P., Robert, D. Modified $TiO_2$ for environmental photocatalytic applications: a review. Ind. Eng. Chem. Res. 2013, 52 (10): 3581.

[5] Hoang, S., Guo, S., Hahn, N.T. Visible light driven photoelectrochemical water oxidation on nitrogen–modified $TiO_2$ nanowires. Nano Lett. 2012, 12(1): 26–32.

[6] Mamane, H., Horovitz, I., Lozzi, L., Camillo. The role of physical and operational parameters in photocatalysis by N–doped $TiO_2$ sol–gel thin films. Chem. Eng. J. 2014, 257(6): 159–169.

[7] Ramchiary, A. and Samdarshi, S.K.. Hydrogenation based disorder–engineered visible active N–doped mixed phase titania. Sol. Energy Mater. Sol. Cells 2015, 134: 381 –388.

[8] Powell, M.J., Dunnill, C.W., Parkin, I. P. N–doped $TiO_2$ visible light photocatalyst films via a sol–gel route using TMEDA as the nitrogen source. J. Photoch. Photobio. A 2014, 281(5): 27–34.

[9] Todorova, N., Hishita, S., and Boukos, N. N and N, S–doped $TiO_2$ photocatalysts and their activity in NOx oxidation. Catal. Today 2013, 209 (12): 41–46.

[10] Triantis, T.M. and Fotiou, T. Photocatalytic degradation and mineralization of microcystin–LR under UV–A, solar and visible light using nanostructured nitrogen doped $TiO_2$. J. Hazard. Mater. 2012, S (211–212)(2): 196–202.

[11] Wang, W.N., Ramalingam, B., and Mukherjee, S. Size and structure matter: enhanced $CO_2$ photoreduction efficiency by size–resolved ultrafine Pt nanoparticles on $TiO_2$ single crystals. J. Am. Chem. Soc. 2012, 134(27): 11276–11281.

[12] Burda, C., Lou, Y., Chen, X. Enhanced nitrogen doping in $TiO_2$ nanoparticles. Nano Lett. 2003, 3, (8): 1049–1051.

[13] Niu, P.J., Yan, J.L., Xu, C.Y. First-principles study of nitrogen doping and oxygen vacancy in cubic $PbTiO_3$. Comput. Mater. Sci. 2015, 98: 10–14.
[14] Tang, B., Liu, X., Cao, X. Experimental and theoretical studies on photocatalytic activity of N–doped $TiO_2$ with different concentration. J. Synth. Cryst. 2015, 44(7): 1885–1889.
[15] Pan, H., Zhang, Y.W., Shenoy, V.B., Gao, H. Effects of H–, N–, and (H, N) –doping on the photocatalytic activity of $TiO_2$. J. Phys. Chem. C 2011, 115: 12224–12231.